

Design of a Spatially Constrained Anti-aliasing Filter using Slepian Functions on the Sphere

Usama Elahi*, Zubair Khalid†, Member, IEEE, and Rodney A. Kennedy*, Fellow, IEEE

* Research School of Engineering, The Australian National University, Canberra, ACT 2601, Australia

† School of Science and Engineering, Lahore University of Management Sciences, Lahore, Pakistan

Email: {usama.elahi@anu.edu.au, zubair.khalid@lums.edu.pk, rodney.kennedy@anu.edu.au}

Abstract—In acoustics, the performance of spherical microphone arrays is limited by spatial aliasing due to the production of side lobes in the array beam. Anti-aliasing filters are used for spatial filtering of the signals reducing the aliasing errors produced in the measurements. In this paper, we propose the design of a spatially constrained filter which approximates the unconstrained ideal anti-aliasing filter used in the literature as a weighted sum of concentrated eigenfunctions obtained by solving the Slepian concentration problem on the sphere. Three performance parameters namely white noise gain (WNG), directivity index (DI) and processing loss are employed to compare the performance of proposed filter with the unconstrained ideal filter. We also propose a parameter-constrained filter design by maximizing WNG subject to constraints on the directivity index and processing loss of the proposed filter. We reconstruct the signal using both filters and analyse the error between the two in spatial domain. Results show that for higher band-limits, the proposed filter matches the unconstrained ideal filter in performance.

Index Terms—Microphone arrays, spatial aliasing, spatial filtering, anti-aliasing filters, slepian eigenfunction.

I. INTRODUCTION

In many real world applications, signals are naturally defined on the sphere. Particularly, in acoustics, spherical microphone arrays have been used for sound field analysis [1], sound field recordings [2], [3] and beamforming [4], [5]. In array processing, the spherical harmonics transform (SHT) [6] is used to examine the array performance [5]. At high frequencies, however, the array performance is limited by spatial aliasing [7] as side lobes are generated in the array beam pattern. In literature, there exists certain sampling schemes that provide aliasing free sampling for band-limited array

This work was supported under the Australian Research Council's Discovery Projects funding scheme (Project no. DP170101897). Zubair Khalid is supported by Pakistan HEC 2016-17 NRPU (Project no. 5925).

measurements [8], however, acoustics sound fields such as measurements of sound pressure produced by plane waves are not band-limited on the sphere, giving rise to spatial aliasing at higher frequencies in practice.

In [7], a theoretical analysis of the spherical microphone reveals spatial aliasing as the significant factor impacting the performance of the antenna array. Several approaches to handle the spatial aliasing such as spatial anti-aliasing filters, using sensors with high directivity and reduction of spatial resolution at higher frequencies are presented in [9]. Anti-aliasing filters are deployed to improve the performance of the microphone arrays in [8], where spatial truncation is applied by first designing an unconstrained ideal filter and then applying window functions on unconstrained ideal filter in order to get spatially constrained anti-aliasing filters. In [10], a spatially constrained anti-aliasing filter based on spatial truncation of unconstrained ideal filter by Slepian eigenfunction window obtained as a solution of slepian concentration problem on the sphere [11], [12] is proposed.

In this work, we design a spatially constrained anti-aliasing filter as a weighted sum of band-limited spatially (optimal) concentrated functions. Given the spatial constraints, the proposed filter approximates an unconstrained ideal low-pass filter on the sphere in the least-squares sense. The weights are applied to the band-limited eigenvectors or eigenfunctions obtained by the solution of the Slepian concentration problem on the sphere [11], [12]. The filter obtained as a result of this multiple regression depends on the value of band-limit, L and maximum concentration region known as polar cap parameterized by its central angle θ_c . We choose $N_o < L + 1$ maximally concentrated eigenvectors where we choose N_o such that we only use spatially concentrated functions in the design. We examine the performance of the proposed filter by measuring parameters like white noise gain (WNG), directivity index (DI) [13] and processing loss (γ) [14], and compare the results with the

unconstrained ideal filter. We compare the performance of two filters first by varying polar cap of angle θ_c keeping band-limit, L constant and then varying band-limits keeping polar cap region constant. By putting constraints on the directivity index and processing loss, we propose a parameter-constrained filter design and choose θ_c such that white noise gain of the proposed filter is maximized. Our analysis show that based on the selected design requirements, the proposed spatially constrained anti-aliasing filter matches the unconstrained ideal filter in performance.

The paper is organised as follows. The mathematical background is given in Section II. Sampling scheme used, aliasing function and spatial filtering are reviewed in detail in Section III. The proposed constrained filter designs are discussed in Section IV, where we also analyse the performance of the filter based on WNG, DI and processing loss. Concluding remarks are made in Section V.

II. SPATIAL ALIASING AND FILTERING ON THE SPHERE

A. Signals and systems on the Sphere

We consider complex-valued functions on the unit sphere which form a Hilbert space, $L^2(\mathbb{S}^2)$ equipped with the following inner product [6]

$$\langle g, f \rangle \triangleq \int_{\mathbb{S}^2} g(\theta, \phi) \overline{f(\theta, \phi)} \sin \theta d\theta d\phi, \quad (1)$$

where $\overline{(\cdot)}$ is the complex conjugate operation and the differential area element on the sphere is $\sin \theta d\theta d\phi$. We parameterize a point on the unit sphere as $(\sin \theta \cos \phi, \sin \theta \sin \phi, \cos \theta) \in \mathbb{S}^2 \subset \mathbb{R}^3$ where $\theta \in [0, \pi]$ represents the co-latitude and $\phi \in [0, 2\pi]$ denotes the longitude. The inner product (1) induces a norm $\|g\| \triangleq \langle g, g \rangle^{1/2}$ and functions with finite induced norms (energy) are referred to as signals on the sphere [6]. We can expand a function $g \in L^2(\mathbb{S}^2)$ as

$$g(\theta, \phi) = \sum_{\ell=0}^{\infty} \sum_{m=-\ell}^{\ell} (g)_{\ell}^m Y_{\ell}^m(\theta, \phi), \quad (2)$$

where $Y_{\ell}^m(\theta, \phi)$ represents the spherical harmonics which form archetype complete orthonormal set of basis functions for $L^2(\mathbb{S}^2)$ for all integer degrees $\ell \geq 0$ and integer orders $m \leq |\ell|$. $(g)_{\ell}^m$ denotes the spherical harmonic Fourier coefficient of degree ℓ and order m and is given by

$$(g)_{\ell}^m \triangleq \langle g, Y_{\ell}^m \rangle = \int_{\mathbb{S}^2} g(\theta, \phi) \overline{Y_{\ell}^m(\theta, \phi)} \sin \theta d\theta d\phi. \quad (3)$$

The signal $g(\theta, \phi)$ is considered as band-limited at degree L if $(g)_{\ell}^m = 0$ for all $\ell > L$. For azimuthally symmetric signal $g(\theta, \phi) = g(\theta)$, $(g)_{\ell}^m = 0, \forall m \neq 0$.

B. Aliasing Function

Spatial aliasing affects the performance of spherical microphone arrays at high frequencies. In the literature, there are sampling schemes which provide aliasing free sampling for band-limited functions on the sphere. The sound pressure, however is not a band-limited function on sphere and hence measurements are affected by spatial aliasing at higher frequencies [3]. A detailed analysis of the nature of aliasing error in spherical microphone arrays is given in [7]. We adopt equiangular sampling scheme proposed in [15] as it requires least number of samples for exact computation of SHT defined in (3) of a band-limited signal on the sphere and use Ω_j to denote the set of equiangular sampling points taken on L isatitude rings. We sample the function (such as sound pressure) by N microphone arrays at positions Ω_j and its spherical coefficients are estimated by using (2) as

$$\begin{aligned} (\hat{g})_{\ell}^m &= \sum_{j=1}^N \omega_j g(\theta_j, \phi_j) \overline{Y_{\ell}^m(\theta_j, \phi_j)}, \\ &= \sum_{\ell'=0}^{\infty} \sum_{m'=-\ell'}^{\ell'} (g)_{\ell'}^{m'} \sum_{j=1}^N \omega_j Y_{\ell'}^{m'}(\theta'_j, \phi'_j) \overline{Y_{\ell}^m(\theta_j, \phi_j)}, \end{aligned} \quad (4)$$

where ω_j are the weights which depend on the sampling scheme chosen and

$$\sum_{j=1}^N \omega_j Y_{\ell'}^{m'}(\theta'_j, \phi'_j) \overline{Y_{\ell}^m(\theta_j, \phi_j)} = \begin{cases} \delta_{\ell\ell'} \delta_{mm'} & \ell, \ell' \leq L, \\ \epsilon_{\ell,m,\ell',m'} & \ell \leq L < \ell', \end{cases} \quad (5)$$

where $\delta_{\ell\ell'} \delta_{mm'}$ represent the Kronecker delta function and $\epsilon_{\ell,m,\ell',m'}$ is the aliasing error.

C. Spatial Filtering and Unconstrained ideal Anti-Aliasing Filter

Let f represents the sound pressure and the measurements are taken by rotating the microphone around the sphere. The spatial filtering can be obtained by using spherical correlation of pressure function f and an azimuthally symmetric spatial filter, denoted by h as [16]

$$F(\alpha, \beta, \gamma) = \int_{\mathbb{S}^2} f(\Omega) \overline{\Lambda(\alpha, \beta, \gamma) h(\Omega)} \sin \theta d\theta d\phi, \quad (6)$$

where $\Omega \in \mathbb{S}^2$ represents the position on the sphere and $\Lambda(\alpha, \beta, \gamma)$ is the rotation operator in $SO(3)$, where α and γ represents rotation along z-axis and β rotation along the y-axis. The spherical correlation in (6) can be re-written as [16]

$$F(\Lambda) = \sum_{\ell=0}^{\infty} \sum_{m=-\ell}^{\ell} \sum_{m'=-\ell}^{\ell} (f)_\ell^m \overline{(h)_\ell^m} D_\ell^{mm'}(\Lambda), \quad (7)$$

where $D_\ell^{mm'}(\Lambda)$ are the wigner-D functions [6], which are basis functions for the fourier transform on the rotation group $SO(3)$. Because of azimuthal symmetry, h is invariant under rotation along the z-axis ($\gamma = 0$), that is, $\Lambda(\alpha, \beta, \gamma) = \Lambda(\alpha, \beta)$, F is mapped to \mathbb{S}^2 as

$$\begin{aligned} F(\alpha, \beta) &= \sum_{\ell=0}^{\infty} \sum_{m=-\ell}^{\ell} (f)_\ell^m \overline{(h)_\ell^0} D_\ell^{m0}(\alpha, \beta, 0), \\ &= \sum_{\ell=0}^{\infty} \sum_{m=-\ell}^{\ell} (f)_\ell^m \overline{(h)_\ell^0} \sqrt{\frac{4\pi}{2\ell+1}} Y_\ell^m(\alpha, \beta), \\ &= \sum_{\ell=0}^{\infty} \sum_{m=-\ell}^{\ell} (F)_\ell^m Y_\ell^m(\alpha, \beta), \end{aligned} \quad (8)$$

where

$$(F)_\ell^m = (f)_\ell^m \overline{(h)_\ell^0} \sqrt{\frac{4\pi}{2\ell+1}}. \quad (9)$$

It can be seen that aliasing error will diminish if such a filter h can be designed which has low or zero values at high frequencies in the harmonic domain. Following (9), an unconstrained ideal anti-aliasing filter can be designed as

$$(h)_\ell^0 = \begin{cases} \sqrt{\frac{2\ell+1}{4\pi}} & 0 \leq \ell \leq L, \\ 0 & \ell > L, \end{cases} \quad (10)$$

and the spatial filter h can be obtained by taking inverse SHT as

$$\begin{aligned} h(\theta, \phi) &= \sum_{\ell=0}^L \sqrt{\frac{2\ell+1}{4\pi}} Y_\ell^0(\theta, \phi), \\ &= \frac{L}{4\pi(\cos \theta - 1)} [P_L(\cos \theta) - P_{L-1}(\cos \theta)]. \end{aligned} \quad (11)$$

Using an unconstrained ideal filter means building such a microphone which has a sensing surface covering the entire sphere which is not cost efficient. Practically, we want such a sensor which is more spatially constrained and cover only a small section of the sphere. In order to experience minimum possible aliasing, it is desirable to

design such a spatially constrained filter whose performance matches an unconstrained ideal filter. A detailed discussion on the importance of filtering in spherical microphone arrays is given in [8], [10].

III. PROPOSED ANTI-ALIASING FILTER

A. Slepian Concentration Problem - Band-limited Eigenfunctions

As a solution of the eigenvalue problem associated with the Slepian concentration problem on the sphere [11], [12], [17], we obtain band-limited functions on the sphere that maximizes the ratio of the energy in the desired polar cap region, parameterized by angle θ_c and is defined as $R_{\theta_c} = \{(\theta, \phi) \in \mathbb{S}^2, 0 \leq \theta \leq \theta_c\}$ to the energy over the whole sphere. The azimuthally symmetric eigenfunctions g with band-limit L and energy concentration within the polar cap of angle θ_c are obtained as a solution of the following algebraic eigenvalue problem [12]

$$\mathbf{K}\mathbf{g} = \lambda \mathbf{g}, \quad (12)$$

where $\mathbf{g} = [(g)_0^0, (g)_1^0, \dots, (g)_L^0]$ is a column vector of size $(L+1)$ containing spherical harmonic coefficients of zero order of g and \mathbf{K} is real and symmetric matrix with dimensions $(L+1) \times (L+1)$ with entries given by

$$\begin{aligned} K_{\ell,\ell'} &= 2\pi \int_0^{\theta_c} Y_\ell^0(\theta, 0) Y_{\ell'}^0(\theta, 0) \sin \theta d\theta, \\ &= \frac{\sqrt{(2\ell+1)(2\ell'+1)}}{2} \sum_{n=\ell-\ell'}^{n=\ell+\ell'} \left(\begin{matrix} \ell & n & \ell' \\ 0 & 0 & 0 \end{matrix} \right)^2 \\ &\times [P_{n-1}(\cos \theta) - P_{n+1}(\cos \theta)], \end{aligned} \quad (13)$$

where the term in the parenthesis are Wigner-3j symbols which are required to be evaluated for the computation of \mathbf{K} . The eigenvalue problem in (12) can also be solved by eigen decomposition of a matrix \mathbf{S} of size $(L+1) \times (L+1)$ commuting it with \mathbf{K} , that is, $\mathbf{KS} = \mathbf{SK}$. \mathbf{S} is a tridiagonal matrix having the following entries [12], [17]

$$\begin{aligned} S_{\ell,\ell+1} &= \frac{(\ell+1)((\ell(\ell+2) - (L)(L+2))}{\sqrt{(2\ell+1)(2\ell+3)}}, \\ S_{\ell,\ell} &= -\ell(\ell+1) \cos(\theta_c), \quad S_{\ell,\ell'} = 0. \end{aligned} \quad (14)$$

The eigen decomposition of \mathbf{S} gives $L+1$ eigenvectors of the form \mathbf{g}_α . Since the eigenvalue problem in (12) is formulated in the spectral domain, each eigenvector represents the spectral domain (spherical harmonic coefficients) of the associated azimuthally symmetric eigenfunction $g_\alpha(\theta)$ in the spatial domain. We have the

following orthonormality and orthogonality relations for the eigenfunctions

$$\mathbf{g}_\alpha'^T \mathbf{g}_\alpha = \langle g_\alpha, g'_\alpha \rangle = \delta_{\alpha\alpha'}, \quad \mathbf{g}_\alpha'^T \mathbf{K} \mathbf{g}_\alpha = \lambda \delta_{\alpha\alpha'}, \quad (15)$$

where $(\cdot)^T$ represents the transpose operation and $0 \leq \lambda_\alpha \leq 1$ associated with the eigenfunction represents a measure of energy concentration of the eigenfunction in the polar cap region R_{θ_c} .

B. Proposed Filter Design

In order to design the proposed spatially constrained anti-aliasing filter, we take the most N_o concentrated eigenfunctions obtained as a solution of the Slepian concentration problem for band-limit L and polar cap region R_{θ_c} . We note that the sum of eigenvalues $N_o = \lceil \frac{(L+1)\theta_c}{\pi} \rceil$ serves as a good measure to approximate the number of concentrated eigenfunctions [12]. We propose to design the band-limited filter \tilde{h} , parameterized by band-limit L and θ_c defining the polar cap region, as a weighted sum of N_o eigenfunctions. We formulate this construction in the harmonic domain as

$$(\tilde{h})_\ell^0 = \beta_1 (\mathbf{g}_1)_\ell^0 + \beta_2 (\mathbf{g}_2)_\ell^0 + \cdots + \beta_{N_o} (\mathbf{g}_{N_o})_\ell^0, \quad (16)$$

where β represents the corresponding weights and are evaluated such that the proposed filter approximates the unconstrained ideal filter in the least-squares sense. Since we use the eigenfunctions that are characterized by both L and θ_c , we note that the proposed filter depends on L and θ_c , that is, $\tilde{h} = \tilde{h}(L, \theta_c)$. The rationale behind the proposed construction is to use spatially concentrated eigenfunctions to approximate the band-limited filter and enabling the control on the spatial resolution θ_c of the filter. We note that we recover the unconstrained ideal filter, that is, $\tilde{h}(L, \pi) = h$, when $\theta_c = \pi$ (the polar cap region is whole sphere $R_\pi = \mathbb{S}^2$).

C. Parameter-constrained Filter Design and Analysis

Using the proposed construction of the filter, we also present a parameter-constrained filter design taking into account the array performance parameters. The performance parameters under study are white noise gain (WNG), directivity index (DI) [13] and processing loss [14]. To maintain consistency in the analysis, we normalise the harmonic coefficients of both the unconstrained ideal and the proposed filter to have unit energy, that is, $\|h\| = \|\tilde{h}\| = 1$. Here we define the performance parameters and compare the performance of the unconstrained ideal and proposed filter based on these parameters under certain settings. Later, we apply constraints on the proposed spatially constrained

anti-aliasing filter and design an optimal parameter-constrained filter that maximizes WNG.

White Noise Gain (WNG): WNG is a measure of the improvement in signal to noise ratio at the array output compared to the array input. Assume an array of band-limit L with $P \geq L^2$ microphones, the WNG with the array looking at the arrival direction (θ_i, ϕ_i) of the plane wave can be written as [13]

$$WNG = \frac{P}{4\pi^2} \frac{\left| \sum_{\ell=0}^L c_\ell (2\ell + 1) \right|^2}{\sum_{\ell=0}^L \frac{|c_\ell|^2}{|b_\ell|^2} (2\ell + 1)}, \quad (17)$$

where c_ℓ is equal to $(\tilde{h})_\ell^0 \sqrt{\frac{4\pi}{2\ell+1}}$ and b_ℓ for the rigid sphere is calculated from [7].

Directivity Index (DI): The directivity index (DI) gives a measure to improved directivity of the array compared to an omnidirectional microphone [13] and can be written as the ratio of the array output in the look direction and the array output integrated over all directions. Assume that the array look direction is $(\theta_i, \phi_i) = (0, 0)$, that is, the z-axis direction, and the directive index can be written as

$$DI = \frac{\left| \sum_{\ell=0}^L c_\ell (2\ell + 1) \right|^2}{\sum_{\ell=0}^L |c_\ell|^2 (2\ell + 1)}. \quad (18)$$

Processing Loss (γ): A certain amount of the signal is lost when a field is filtered. We quantify such processing loss, γ , as

$$\gamma = 1 - (\zeta), \quad \zeta = \sum_{\ell=0}^{L-1} \frac{c_\ell^2}{L}, \quad (19)$$

where ζ is the damping factor which provide information about the extent of dampness in amplitude in the filtering.

1) Analysis: Based on three performance parameters defined previously, we compare the performance of the proposed spatially constrained filter with the unconstrained ideal filter. Fig. 1 compares the performance of the unconstrained ideal filter and the proposed filter designed for band-limit $L = 20$ and polar cap regions, $\pi/18 \leq \theta_c \leq 2\pi/3$. It can be seen that WNG of the proposed filter is better than the unconstrained ideal filter for selected values of θ_c . The directivity index of the proposed filter approaches the value attained by the unconstrained ideal filter as θ_c increases from 0 to π . Processing loss (γ) of the unconstrained ideal filter is zero and it can be seen that processing loss approaches

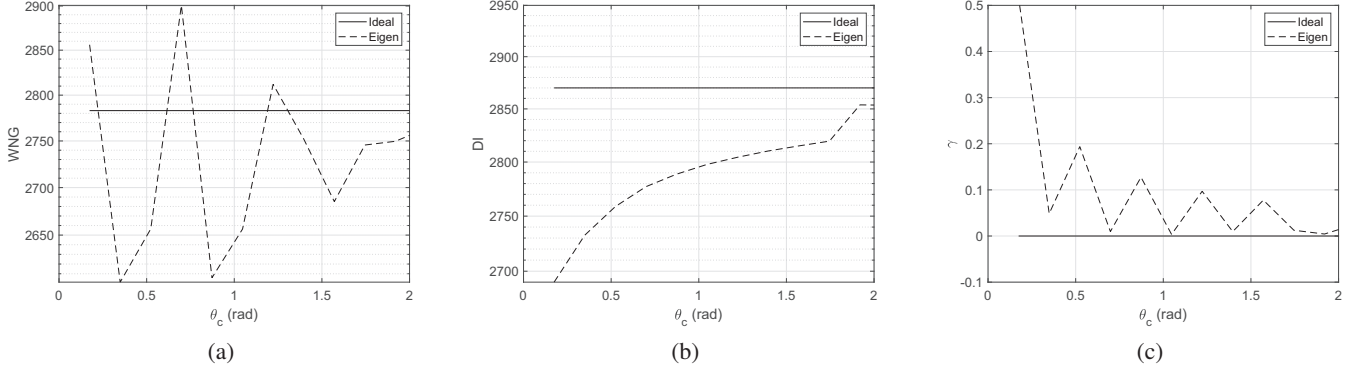


Fig. 1: Performance parameters, (a) white noise gain (WNG), (b) directivity index (DI) and (c) processing loss (γ), of unconstrained ideal and proposed spatially constrained filter having fixed band-limit, $L = 20$ and plotted for random polar cap regions of angle, $\pi/18 \leq \theta_c \leq 2\pi/3$.

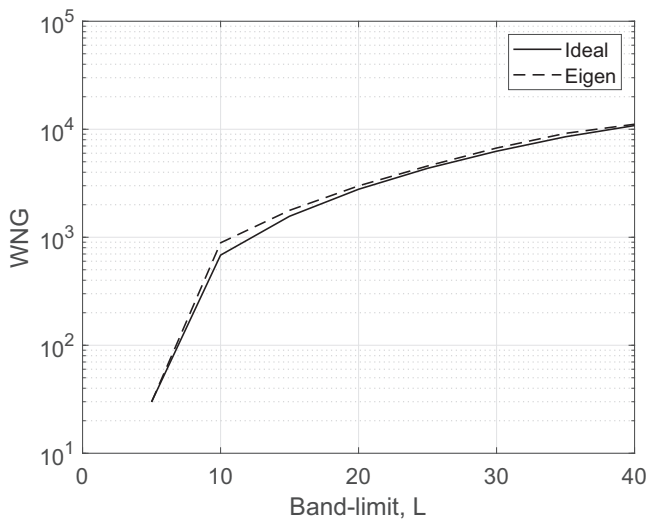


Fig. 2: The optimized WNG of the proposed eigen filter against unconstrained ideal filter, plotted for chosen optimized polar cap, $(\hat{\theta}_c)$ for $5 \leq L \leq 40$.

the unconstrained ideal filter for some values of θ_c . In the following, we propose a constrained filter design where we find the optimal value of θ_c for which the proposed filter behaves as ideal filter.

2) *Constrained Filter Design:* In the constrained design of the filter, $\tilde{h}(L, \theta_c)$, we find θ_c by formulating the following optimization problem

$$\begin{aligned} & \underset{\tilde{h}}{\text{maximize}} && WNG \\ & \text{subject to} && \zeta \geq 0.99, \\ & && DI = \delta_L, \end{aligned} \quad (20)$$

where δ_L denotes the directivity index of unconstrained ideal filter for a band-limit, L . Since the optimization problem in (20) is intractable, we solve it numerically and choose such θ_c for which

$$|\sum_{\ell=0}^{L-1} c_{\ell pr.} (2\ell + 1)|^2 > (0.99L),$$

$$\delta_L \sum_{\ell=0}^{L-1} |c_{\ell pr.}|^2 (2\ell + 1) > |\sum_{\ell=0}^{L-1} c_{\ell uci.} (2\ell + 1)|^2, \quad (21)$$

where $pr.$ and $uci.$ are representing proposed and unconstrained ideal filters respectively. In (21) and (21), we put constraints on the processing loss and take the directivity index of the proposed filter to be equal to that of the unconstrained ideal filter as our design requirements are limited to maximizing the WNG. After putting constraints and optimizing WNG, we have a filter which has a better WNG compared to the unconstrained ideal filter for any band-limit L and the optimized polar cap, $\hat{\theta}_c$ as shown in Fig. 2. To conclude the analysis, we also reconstruct the signal (sound pressure in case of microphone arrays [10]) on the sphere after filtering using the unconstrained ideal filter and the proposed spatially constrained filter. We calculate the error between the two filtered signals on sphere and plotted the results in spatial domain in Fig. 3 for a fixed polar cap $\theta_c = \pi/2$ and different band-limits, $L = 20, 40, 60$. As we increase the band-limit, greater number of eigenvectors, N_o are used, approximation becomes better and hence the proposed constrained filter approaches the unconstrained ideal filter in performance.

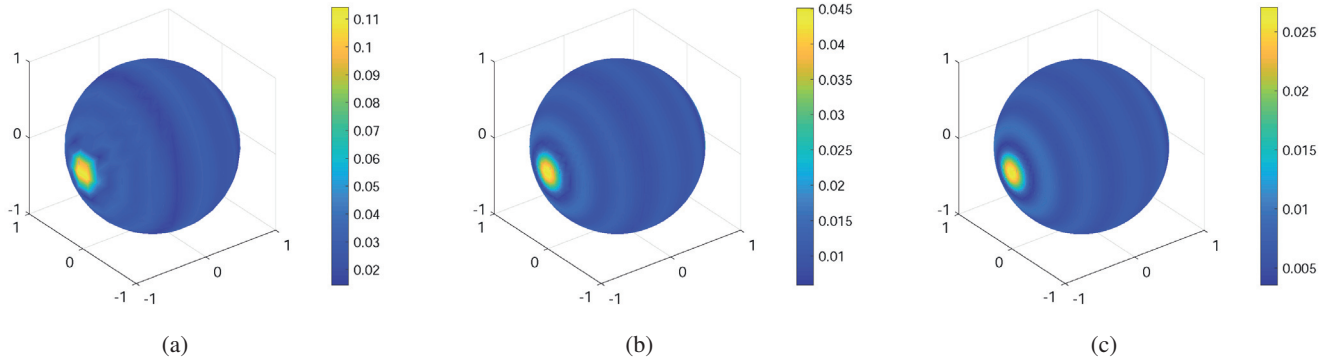


Fig. 3: Error between the signals filtered by the unconstrained ideal filter and the proposed spatially constrained filter for $\theta_c = \pi/2$ and band-limit, (a) $L = 20$, (b) $L = 40$ and (c) $L = 60$.

IV. CONCLUSIONS

In this paper, we have proposed the design of a spatially constrained anti-aliasing filter by utilizing the spatially concentrated eigenfunctions obtained as a solution of Slepian concentration problem on the sphere. The proposed filter depends on the spatial resolution parameter θ_c and the harmonic band-limit L . Having control on both the spatial resolution and harmonic band-limit allows us to take into account the performance parameters of the filter in the design and analysis of the filter. We have also compared the performance of the proposed filter with the unconstrained ideal filter by employing the three performance parameters, white noise gain (WNG), directivity index (DI) and processing loss. We have also proposed a parameter-constrained filter design that maximizes WNG with constraints on the other performance parameters. Finally, the reconstruction error analysis shows that the proposed spatially constrained filter behave like an unconstrained ideal filter for large band-limits and greater number of Slepian eigenvectors.

REFERENCES

- [1] J. Meyer and T. Agnello, "Spherical microphone array for spatial sound recording," in *Audio Engineering Society Convention 115*. Audio Engineering Society, 2003.
- [2] G. Weinreich and E. B. Arnold, "Method for measuring acoustic radiation fields," *The Journal of the Acoustical Society of America*, vol. 68, no. 2, pp. 404–411, 1980.
- [3] T. D. Abhayapala and D. B. Ward, "Theory and design of high order sound field microphones using spherical microphone array," in *2002 IEEE International Conference on Acoustics, Speech, and Signal Processing*, vol. 2, May 2002, pp. II-1949–II-1952.
- [4] J. Meyer and G. Elko, "A highly scalable spherical microphone array based on an orthonormal decomposition of the sound-field," in *2002 IEEE International Conference on Acoustics,* Speech, and Signal Processing, vol. 2, May 2002, pp. II-1781–II-1784.
- [5] D. L. Alon and B. Rafaely, "Beamforming with optimal aliasing cancellation in spherical microphone arrays," *IEEE/ACM Transactions on Audio, Speech, and Language Processing*, vol. 24, no. 1, pp. 196–210, Jan 2016.
- [6] R. A. Kennedy and P. Sadeghi, *Hilbert Space Methods in Signal Processing*. Cambridge, UK: Cambridge University Press, Mar. 2013.
- [7] B. Rafaely, "Analysis and design of spherical microphone arrays," *IEEE Transactions on speech and audio processing*, vol. 13, no. 1, pp. 135–143, 2005.
- [8] B. Rafaely, B. Weiss, and E. Bachmat, "Spatial aliasing in spherical microphone arrays," *IEEE Transactions on Signal Processing*, vol. 55, no. 3, pp. 1003–1010, 2007.
- [9] J. Meyer and G. W. Elko, "Handling spatial aliasing in spherical array applications," in *Hands-Free Speech Communication and Microphone Arrays, 2008. HSCMA 2008*. IEEE, 2008, pp. 1–4.
- [10] U. Elahi, Z. Khalid, and R. A. Kennedy, "Spatially constrained anti-aliasing filter using slepian eigenfunction window on the sphere," in *2018 12th International Conference on Signal Processing and Communication Systems (ICSPCS)*, Dec 2018, pp. 1–6.
- [11] Z. Khalid, S. Durrani, P. Sadeghi, and R. A. Kennedy, "Spatio-spectral analysis on the sphere using spatially localized spherical harmonics transform," *IEEE Trans. Signal Process.*, vol. 60, no. 3, pp. 1487–1492, Mar. 2012.
- [12] F. J. Simons, F. A. Dahlen, and M. A. Wieczorek, "Spatiospectral concentration on a sphere," *SIAM Rev.*, vol. 48, no. 3, pp. 504–536, 2006.
- [13] B. Rafaely, "Phase-mode versus delay-and-sum spherical microphone array processing," *IEEE signal processing Letters*, vol. 12, no. 10, pp. 713–716, 2005.
- [14] B. Devaraju, *Understanding filtering on the sphere: experiences from filtering GRACE data*, 2015.
- [15] J. D. McEwen and Y. Wiaux, "A novel sampling theorem on the sphere," *IEEE Trans. Signal Process.*, vol. 59, no. 12, pp. 5876–5887, Dec. 2011.
- [16] P. J. Kostelec and D. N. Rockmore, "FFTs on the rotation group," *J. Fourier Anal. and Appl.*, vol. 14, pp. 145–179, 2008.
- [17] Z. Khalid, R. A. Kennedy, and S. Durrani, "On the choice of window for spatial smoothing of spherical data," in *Acoustics, Speech and Signal Processing (ICASSP), 2014 IEEE International Conference on*. IEEE, 2014, pp. 2644–2648.